International Journal of Impact Engineering 178 (2023) 104606

Contents lists available at ScienceDirect

International Journal of Impact Engineering

journal homepage: www.elsevier.com/locate/ijimpeng

Quasi-static and impact behaviour of foam-filled graded auxetic panel

Nejc Novak [a,*], Hasan Al-Rifaie [b], Alessandro Airoldi [c], Lovre Krstulović-Opara [d], Tomasz Łodygowski [b], Zoran Ren [a], Matej Vesenjak [a]

[a] Faculty of Mechanical Engineering, University of Maribor, Maribor, Slovenia
[b] Faculty of Civil Engineering and Transport, Poznan University of Technology, Poznan, Poland
[c] Department of Aerospace Science and Technology, Politecnico di Milano, Milano, Italy
[d] Faculty of Electrical Engineering, Mechanical Engineering and Naval Architecture, University of Split, Split, Croatia

ARTICLE INFO

Keywords:
Cellular materials
Auxetic panel
Foam-filled
Polyurethane foam
Crash absorber
Drop test
Experimental testing
Computational modelling

ABSTRACT

Cellular structures (in general) and auxetic topologies (in particular) have excellent energy-dissipation characteristics and can be used as lightweight impact-energy absorbers. This paper aims to experimentally and computationally examine the behaviour of novel re-entrant auxetic graded aluminium panels filled with polyurethane foam in an auxetic pattern. The performance is compared with 3 non-graded, 1 graded and 2 foam-filled graded panels. The 6 compared auxetic panels share the same basic geometry but vary in the sheet thickness and the addition of polyurethane foam. The auxetic panels were built by corrugating and gluing 12 aluminium sheets. The material properties of the used aluminium sheets and foam were determined with standard mechanical testing. Detailed quasi-static and dynamic drop tests were conducted and compared with a non-linear computational model. The stress-strain relationships, deformation patterns, specific energy absorption, crash force efficiency and Poisson's ratio were comprehensively evaluated. Foam-filled panels revealed higher specific energy absorption and more stable deformation than non-filled panels. The developed computational models successfully describe mechanical and deformation behaviour and can be used for future virtual testing of other configurations.

1. Introduction

Cellular sandwich panels usually have two stiff plates and a crushable low-density core in-between [1]. They have become widely used in engineering due to their excellent properties, in terms of lightweight, strength-to-weight ratios, and impact energy absorption, including high-rise buildings, aerospace engineering, automotive industry, defensive solutions, and other protective structures [2]. Sandwich panels with a cellular metallic core can dissipate significant dynamic energy through plastic deformation under impact or blast loading [3]. The cores can be metal foams with regular or irregular topologies or auxetic metamaterials [4,5].

Aluminium is most frequently used to create metallic foams (aluminium foams) with open or closed cells and varying properties [6–10]. Experimental and computational investigations demonstrated high blast energy absorption of metallic foams. However, it is challenging to optimise foam properties for the applied load in practical applications due to inherent irregularity in cell structure. Peroni et al. [10] showed that large density scatter and material anisotropy are the main issue in designing aluminium foams.

Regular topologies, e.g. triangular, rectangular, trapezoidal or hexagonal (also called honeycomb), are alternatives as their behaviour can be tuned to the specific engineering application. For instance, honeycomb structures are used in many protective structures due to their energy absorption and impact resistance properties [11–14]. Their mechanical properties and shock/impact response was studied analytically [15,16], numerically [17–19] and experimentally [20,21].

The state-of-the-art review has shown that auxetic metamaterials provide improved energy dissipation compared to conventional cellular topologies [22–24]. The auxetic characteristic (negative Poisson's ratio) can be either naturally occurring (from the substance itself) or artificially created (changing the geometry on the micro-structure level). The rarely used α-cristobalite silicon dioxide is an example of a naturally occurring material with a negative Poisson ratio [25]. Double arrowhead, re-entrant, chiral, and rotating rigid units are a few examples of cellular geometries that exhibit auxetic behaviour [26,27]. They are

* Corresponding author.
E-mail address: n.novak@um.si (N. Novak).

https://doi.org/10.1016/j.ijimpeng.2023.104606
Received 25 October 2022; Received in revised form 28 March 2023; Accepted 9 April 2023
Available online 10 April 2023

employed in developing metallic auxetic cellular metamaterials, which have a variety of aerospace, biomedicine, and military applications [28]. Auxetic structures and their applications have been well discussed in several scientific manuscripts and review studies [29–33].

Auxetic sandwich panels have shown improved flexural response [34], damage localisation [35,36], energy absorption [37–39] and indentation resistance [40–42] under quasi-static and impact dynamics. It is noteworthy that 3D auxetic structures have been developed [43] in the form of an auxetic frame [44], multi-pod lattice [45], or bow-tie elements [46]. However, complex procedures are needed to create a 3D auxetic structure [43,47] due to current technological constraints. On the contrary, the 2D auxetic structures can be produced relatively easy by profile-rolling/corrugating metal sheets [39,48] or by additive manufacturing [49–51]. Only small-scale auxetic topologies can be fabricated using relatively expensive 3D printing [52]. The sandwich panels with a corrugated core have been suggested as an appealing cheaper alternative for larger auxetic structures, which by design also assure high longitudinal stretching, shear strength, and energy absorption ability [53–55]. The corrugated layers are created using a folding technique and can be welded/glued together to create a comparatively inexpensive core [48]. Similar panels were also fabricated using riveting and tested under blast loading conditions recently [56].

The 2D re-entrant cell topology was used in this study due to its comparatively straightforward geometry and less expensive fabrication compared to alternative auxetic topologies. Additionally, studies in this area indicate that the re-entrant auxetic topology potential needs to be further explored [37]. The investigation of dynamic crushing of cellular materials is often carried out using computational finite element analysis tools [57,58] since experimental procedures are way more expensive [37].

Some recent studies advise adopting sandwich panels with graded layers of non-uniform thicknesses to account for various impact loading conditions [52,59]. For example, Li et al. [60] highlight the importance of graded core and conclude that "*graded sandwich panels, especially for relative density descending core arrangement, would display a better blast resistance than the ungraded ones*". Therefore, graded sandwich panels were also considered in this study.

Foam-filled sandwich panels are widely employed in building construction due to their lightweight qualities, load-bearing capabilities, acoustic insulation, corrosion resistance, and wear resistance. However, this type of sandwich panel cannot bear extreme loads due to either shear failure of the foam core or delamination between the face sheet and the core [61]. Hence, researchers have investigated the behaviour of foam insertion in cellular metals [62,63]. Usta et al. [61] compares the high-velocity impact behaviour of two sandwich panels with polyurethane (PU) foam core and 3D-printed plastic re-entrant auxetic core. Experimental tests with an air gas gun and computational modelling showed that the re-entrant core has higher specific energy absorption (SEA) than the foam core [61]. In Ren et al. [64], a hollow auxetic tube was filled with rigid PU foam to enhance energy absorption. The results show that the overall absorbed energy is larger than the sum of single foam and hollow auxetic tube under compression [64], which reflects the potential benefits of PU foam in auxetic cellular metals. Haque Faisal et al. [65] studied the effect of fillers on the performance of re-entrant auxetic sandwich structures. Core cells were filled with silly putty and polyvinyl chloride (PVC) foam. The study concludes that filling the auxetic cells with soft materials reduced the stress concentration and decreased energy absorption [65] . For localised impact, Airoldi et al. [66] propose an innovative concept for auxetic foam-filled energy absorbers. They consist of a 3D-printed polymeric hexa-chiral frame that is filled with open-cell soft polyurethane foam. The absorbers were tested experimentally and numerically and the results showed that foam filler can provide significant improvements to the specific energy absorption and load uniformity ratio [66].

This paper aims to experimentally and numerically examine the behaviour of a novel re-entrant graded aluminium panel filled with PU foam in an auxetic pattern. The performance is assessed based on quasi-static and dynamic drop tower experiments supported by advanced non-linear finite element modelling.

2. Materials and methods

2.1. Geometry and fabrication of auxetic panels

Six different auxetic panels (APs) were considered in this research, listed in Table 1. All the panels have the same geometry with six re-entrant auxetic layers, built by corrugating and gluing twelve aluminium sheets. Fig. 1 shows the geometry of the fabricated auxetic panels, which was taken from a parametric study done by Al-Rifaie and Sumelka [52]. The unit cells has a width ($L1$) of 40 mm and a height (H) of 30 mm with $L = 17.3$ mm (Fig. 1a,b). The overall dimensions of the auxetic panel are shown in Fig. 1. The height is not provided since the auxetic panel's total height depends on the sheets' thickness and ranges from 189.6 mm in the case of AP 0.8 mm to 194.4 mm in the case of AP 1.2 mm (where 0.8 mm and 1.2 mm are the thicknesses).

The six built auxetic panels vary in the sheet thickness and the addition of PU foam. The first three non-graded auxetic panels have a uniform corrugated sheet thickness throughout the whole panel of 0.8 mm, 1.0 mm and 1.2 mm, respectively. The graded auxetic panel was fabricated with varying sheet thicknesses. The two auxetic layers at the bottom have a sheet thickness of 0.8 mm, the two auxetic layers in the middle have a sheet thickness of 1 mm, and the two auxetic layers at the top have a sheet thickness of 1.2 mm. The last two graded samples were filled with the PU foam as a full-filled graded panel (FFG) and auxetic-filled graded panel (AFG) and are shown in Figs. 1e-f. The AFG configuration was chosen in order to introduce the multi scale auxetic behaviour of the panels, where the filling itself introduces the auxetic effect. At least two samples of each group were tested to determine the representative response in each experimental testing type.

The auxetic panel's production method was adopted from Remennikov et al. [48], who produced the first large-scale auxetic panels. Corrugated sheets made of aluminium alloy (AW-5754, T111, Impol, SLOVENSKA BISTRICA, Slovenia) with density $\rho_s = 2660$ kg/m^3 were used to create the 25 auxetic cores. The corrugated sheets were then assembled to auxetic panels with epoxy adhesive LOCTITE® EA 9466 (DÜSSELDORF, Germany), as shown in Figs. 1c-d. At room temperature, the glue hardens, forming a solid bond with good peel resistance and shear strength. It is made for uses where a long lifespan and robust binding strength are necessary.

The FFG and AFG samples were filled with commercially available PU foam (Tekapur low expansion, TKK d.o.o., Slovenia) with resulting density of 19.3 kg/m^3. The foam was applied to the empty cells directly from the spray and was left to harden at room temperature for 24 h. The weight of the FFG and AFG panels was increased by 10.4% and 5.5%, respectively, compared to the non-filled graded panel, as shown in

Table 1
Weight and porosity of the 6 considered Auxetic Panels (AP).

Absorber type	Comment	Number of samples	Weight [kg]	Porosity [%]
AP 0.8 mm	Uniform panel with 0.8 mm thick sheets	5	1.36	91.8
AP 1.0 mm	Uniform panel with 1.0 mm thick sheets	5	1.69	90.1
AP 1.2 mm	Uniform panel with 1.2 mm thick sheets	5	1.96	88.5
Graded	Graded panel with 0.8 – 1.2 mm thick sheets	6	1.63	90.1
FFG	Graded panel fully-filled with PU foam	2	1.80	89.0
AFG	Graded panel auxetically-filled with PU foam	2	1.72	89.5

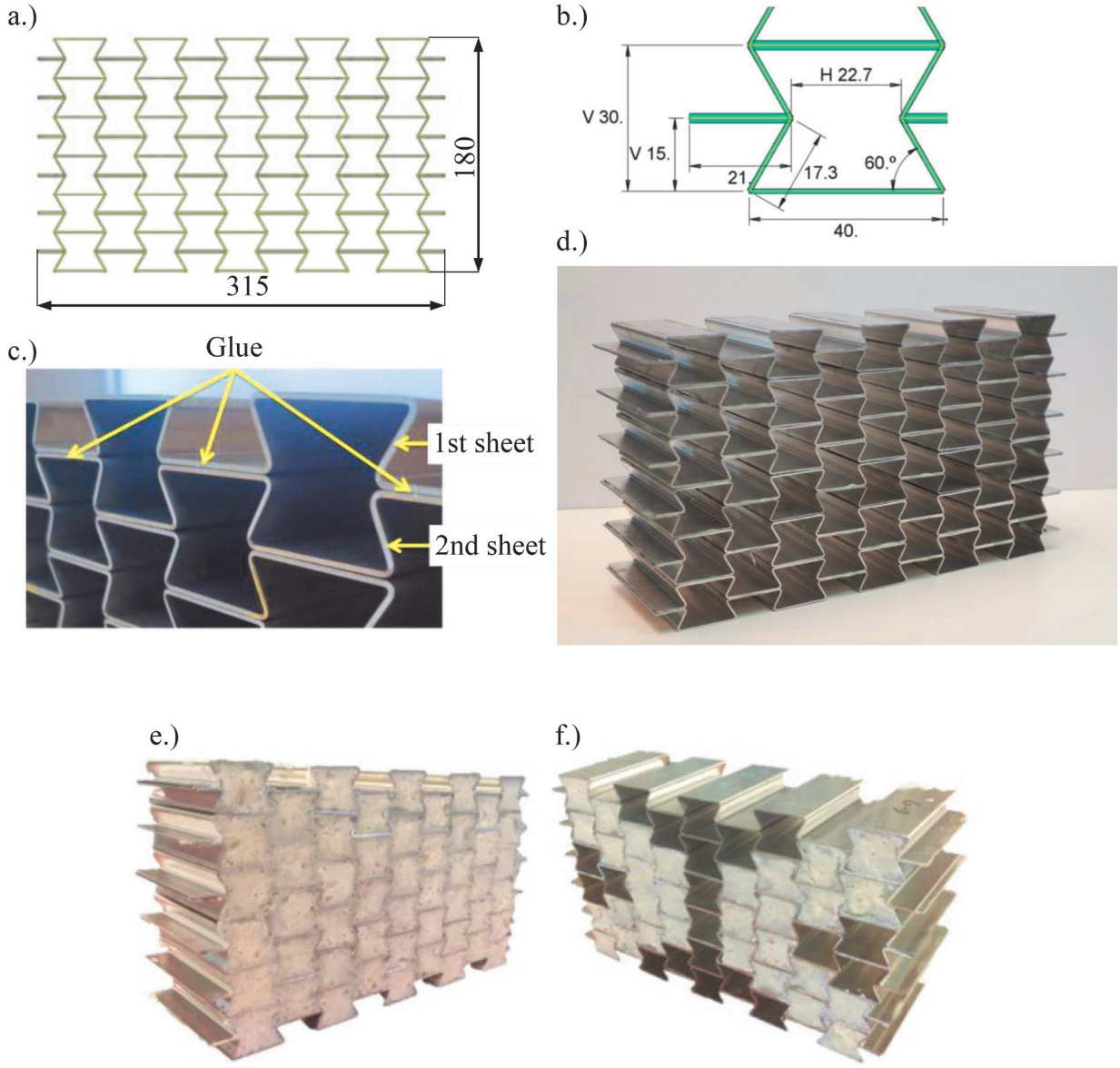

Fig. 1. Geometry of the auxetic panel: a.) auxetic panel dimensions (depth: 100 mm), b.) unit cell dimensions, c.) positioning of panels, d.) fabricated auxetic panel, e.) fabricated full-filled graded panel (FFG) and f.) fabricated auxetic-filled graded panel (AFG).

Table 1. The porosity of the panels is provided in Table 1. It was calculated by dividing the weight of the panel with the weight calculated by volume of panel and density of aluminium. The volume was calculated from boundary box area of the panel (315 mm width x 180 mm height) and the depth of the panel (100 mm).

2.2. Material testing

To determine the precise mechanical properties of the used aluminium alloy, a series of standard tensile tests were carried out using the universal testing apparatus INSTRON® 8801 at constant loading velocities of 0.1 mm/s (quasi-static testing, strain rate of 0.002 s^{-1}) and 284 mm/s (dynamic testing, strain rate of 5.68 s^{-1}). The 3 sets of dog-bone samples following the DIN50125 standard with thicknesses of 0.8 mm, 1.0 mm, and 1.2 mm were tested, where a clip-on extensometer with an initial length of 50 mm. The results are shown in Section 3.1 as an average response of each set of samples. The foam testing was carried out using a servo hydraulic MTS 810 quasi-static test system at quasi-static (2 mm/min, strain rate of 0.001 s^{-1}) and dynamic crosshead velocity (250 mm/s, strain rate of 8.33 s^{-1}). The samples were cut from a larger PU foam panel and prepared as test cubes with dimensions 30 mm × 30 mm × 30 mm. The PU foam panel was fabricated with spraying the PU foam in the container, which was not constrained at the top, mimicking the fabrication procedure of the FFG and AFG. The cubes were compressed between two steel pads connected to the fixed and moving heads of the MTS system.

2.3. Quasi-static and drop tower testing of auxetic panels

The quasi-static testing of auxetic panels was performed on the universal testing machine Instron INSTRON 8801 with a position-controlled crosshead rate of 0.5 mm/s. The nominal stress-strain responses were calculated using the initial dimensions of the samples. Furthermore, the drop tower testing was carried out, consisting of a drop sledge with variable masses guided by two 6 m tall columns. A steel plate was fixed to the sledge to serve as the impacting surface to the top of the auxetic panel specimens. The specimens were positioned on a steel base. The total weight of the impacting mass was 99.5 kg, while the loading velocity of 10 m/s was achieved, which resulted in 4975 J energy of the impact. Two sledge-mounted uniaxial piezoresistive accelerometers

Kilster M64C-2000 with a measuring range of 2000 g and an accuracy of ± 2% up to 3000 Hz were used. The impacts were recorded using a Phantom VEO E-310 L camera, with a capability of 3260 fps at a resolution of 1280 px × 800 px. The acquisition was managed through an Iotech Strainbook/616 measurement system with a WaveView software. The CFC180 filter was used to filter the raw experimental data from drop tower testing, Fig. 2.

Two-dimensional digital image correlation - DIC (GOM Correlate 2019) was applied to determine incremental transverse and axial strains during compression tests, which were used to calculate the Poisson's ratio (PR). The displacements were measured in 7 discrete points on each edge of the sample (Fig. 14a). Average displacements were then used for Poisson's ratio calculations. To prevent any contact and boundary effects on the results, locations near the compression plates were excluded from the examination of transverse displacements.

3. Experimental results

3.1. Material testing of aluminium material and PU foam

The experimental results of base aluminium material testing are shown in Fig. 3a. The results show low strain rate sensitivity at analysed loading velocities and very comparable mechanical responses of 0.8 mm and 1.0 mm thickness sheets. The maximum and average standard deviations of the responses were calculated to be 19.58 and 12.05, respectively. Young's modulus was determined at 63,177 MPa. The Poisson's ratio of 0.33 was assumed from the literature [67]. For the computational simulations of PU foam, the equivalent simplified relationship was used to achieve better convergence and more-stable computational simulations. The simplified description of the mechanical response used in the material (constitutive) model, is given in Table 2.

The experimental testing of the foam (Fig. 3b) shows a typical response of the cellular structure, where the densification follows the initial elastic stage and plateau stress. Significant strain rate sensitivity was also observed in the experimental tests.

3.2. Quasi-static testing of auxetic panels

Fig. 4 shows the deformation process of quasi-static testing uniform and graded auxetic panels. The uniform samples (Fig. 4a) deform primarily in the area of the shear planes, which is followed by densification. It can also be observed that the glue does not fail even at full densification. The deformation mode in the case of graded auxetic panel changes compared to the uniform auxetic panel. The deformation starts in the area where the sample is less stiff (thinnest sheets) and then continues at the thicker sheets.

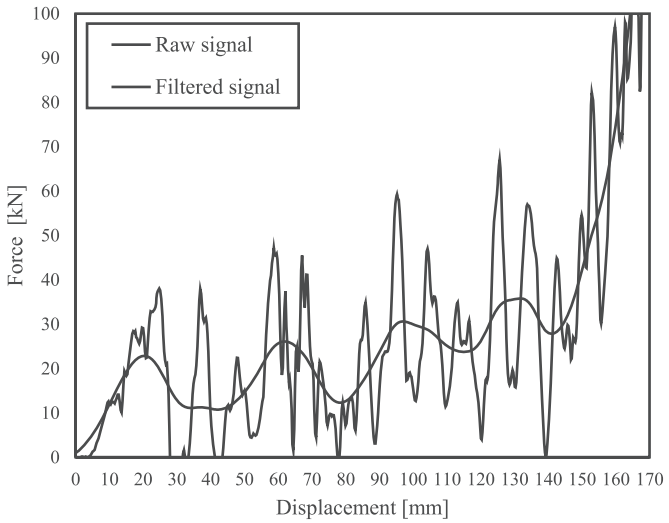

Fig. 2. Filtering of experimental data from drop tower testing.

3.3. Drop tower testing of auxetic panels

The results of drop tower testing are shown in Fig. 5. The uniform (Fig. 5a) and graded (Fig. 5b) auxetic panels have the same deformation behaviour as in the case of quasi-static loading (Fig. 4). The graded auxetic panel shown in Fig. 5b has the thinnest sheets at the top, while the auxetic panel, in the case of quasi-static testing (Fig. 4b), had the thinnest sheets at the bottom. Also, the other specimen orientation was tested, and there was no influence on the mechanical and deformation response since the relatively low loading velocities do not initiate the transition or shock mode response [68].

The deformation behaviour of AFG and FFG samples is shown in Fig. 6. Adding the foam to the auxetic panel does not change the global deformation behaviour, which remains the same as in the case of empty auxetic panels through the entire deformation. Since the PU foam used as filler is very porous and ductile, it densifies and gains significant stiffness at high deformation rates inside the auxetic panel's pores.

Due to the repeatability and low scatter of the experimental results only the average mechanical responses of non-filled and foam-filled auxetic panels are shown in Fig. 7. In the case of non-filled auxetic panels, the mechanical responses reach higher peak stress in the case of dynamic loading using the drop tower. After that initial peak, the stiffness is decreased compared to quasi-static loading, which is more prominent with increasing thickness of the sheets (1.2 mm). This can be consequence of the softer base material of the thicker sheets (Fig. 3a). The initial stiffness is achieved, while the following bending deformation of the panel's walls is more prominent and therefore provides larger stiffness decrease than in the case of panels with thinner sheets. In the case of foam-filled auxetic panel, the behaviour is the same, but when adding the PU foam to the auxetic panel, the stiffness increases.

3.4. Analysis of the experimental results

The specific energy absorption (SEA) was calculated at 30 and 40% strain (the displacement of 57 mm and 76 mm) as:

$$SEA = \frac{\int_0^{\varepsilon} \sigma d\varepsilon}{\rho},$$

where σ is stress, ε strain and ρ density.

The crash force efficiency (CFE) was calculated as:

$$CFE = \frac{\sigma_{aver}}{\sigma_{max}},$$

where σ_{aver} and σ_{max} are the average and maximum mechanical responses up to 40% strain. The SEA and CFE values of all analysed auxetic panel samples are shown in Fig. 8.

The SEA increases from 30% to 40% of strain in all analysed cases, which is expected, since there is more energy absorbed at the larger strains. The increase of the SEA is more pronounced in the case of FFG and AFG panels, which is consequence of more progressive platau, where the stiffness is increasing faster than in the case of empty panels. It is interesting to note that the SEA of auxetic panels increases with the thickness of the corrugated sheet. Even though the mass of the panel rises as well. With sheet thickness increasing from 0.8 mm to 1 mm, the auxetic panel mass increases by 25%, and its SEA by 23%. The same can be observed for the thickness increase of the sides from 1 mm to 1.2 mm. Again, the ability to absorb energy increases more than its mass; consequently, its SEA increases by 29%. The value of the SEA of the graded absorber is 22% lower than that of the 1 mm thick absorber, despite its average sidewall thickness being the same. In general, the SEA increases in dynamic testing compared to quasi-static, which is not

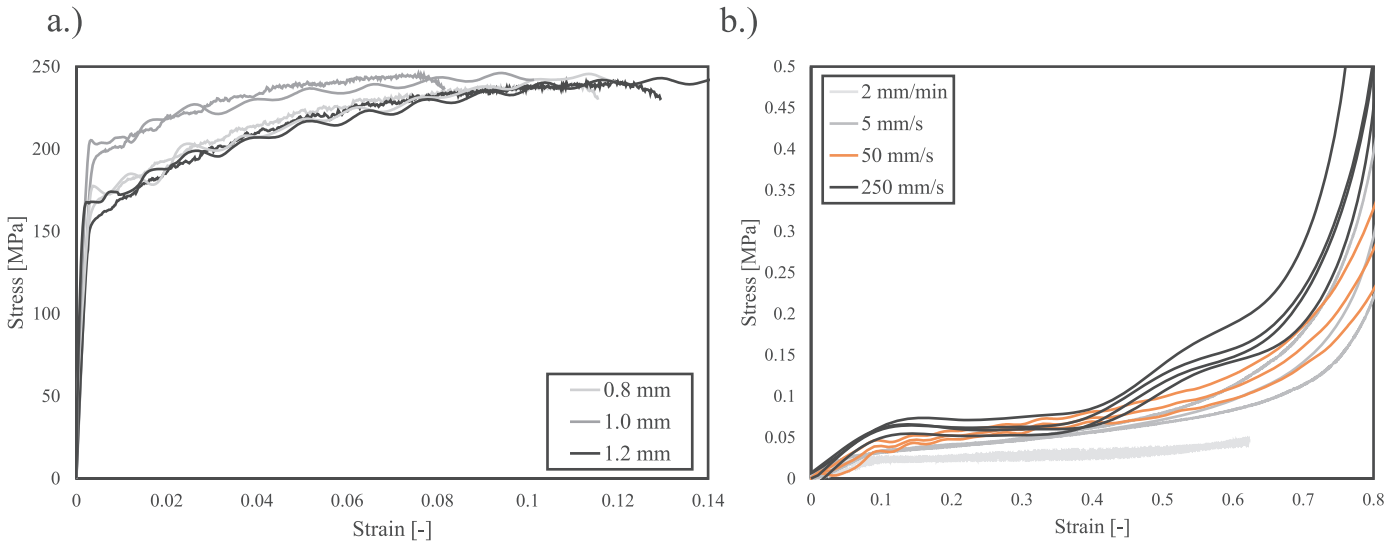

Fig. 3. Material testing of aluminium material and PU foam. a) average experimental results of aluminium tensile tests (solid lines quasi-static testing – 0.01 mm/s, dashed lines dynamic testing – 284 mm/s), b) compression tests of PU foam cubes at different loading velocities (each sample shown with dotted lines).

Table 2
Material models parameters.

AW 5754 (MAT_024) Density	Young's modulus	Poisson's ratio	Hardening definition (ε_{pl}, σ)			
[kg/m^3]	[MPa]	[-]	[-, MPa]			
2660	63,170	0.33	0, 172	0.04, 219	0.08, 235	0.11, 239
PU foam (MAT_063)						
23.3	5.02	0	Simplified experimental curve			

the case only for the panel with 1.2 mm thickness. The dynamic SEA increases the most when compared to quasi-static in the graded sample. The graded foam-filled samples were only dynamic tested. The SEA of foam-filled samples increases up to 23% in the FFG and 9% in the AFG sample compared to the non-filled graded sample.

The CFE values are in general higher at 30% strain, especially is the difference observed in the case of FFG and AFG panels. This is due to the beforementioned increasing nature of plateau. The CFE was approximately 80% for 0.8 mm and 1.0 mm thicknesses and 75% for 1.2 mm thicknesses. This could be anticipated since the absorbers differ only in the sides' thickness, which equally affects the average and maximum pressure load. The CFE is slightly lower for the graded absorber (63%), which is expected, as it consists of panels of different thicknesses, which gradually deform. The CFE in the case of dynamic testing is decreased, while the CFE of the graded sample under dynamic loading is superior compared to others. Different load intensity to deform different parts of the absorber is one of the purposes of using a graded absorber. The thickest panels deform significantly only after 80 mm of displacement, so it makes sense to calculate the graded absorber's mechanical characteristics, considering the results up to 120 mm of displacement to capture the behaviour of all three types of panels. If we increase the degree of deformation at which SEA is calculated from 40% to 66.7% (120 mm displacement), the largest difference occurs with the graded absorber since thicker panels are deformed at higher degrees of deformation, which can absorb more energy. In proportion to the increased absorbed energy, the SEA increases as the degree of deformation increases. However, the CFE is lower than the results at 40% deformation.

4. Computer simulations

4.1. Computational model

The computational simulations were performed using the LS-DYNA software. The geometry of the finite element (FE) model is shown in Fig. 9a. The model was discretised with 5 mm fully-integrated shell finite elements with 5 through-thickness integration points, determined by a convergence study. The glue between the panels was not considered in the model since the adhesive joints did not fail during the experimental tests. The single layer of shell elements was therefore used in the

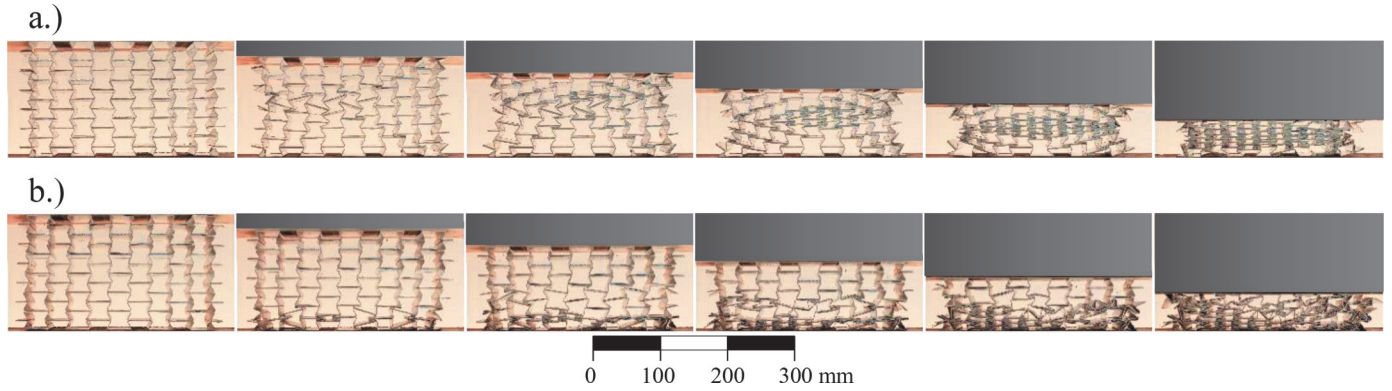

Fig. 4. Quasi-static deformation behaviour of two auxetic panels at different displacements (increments of 25 mm each), a) uniform AP 1.0 mm and b) graded panel.

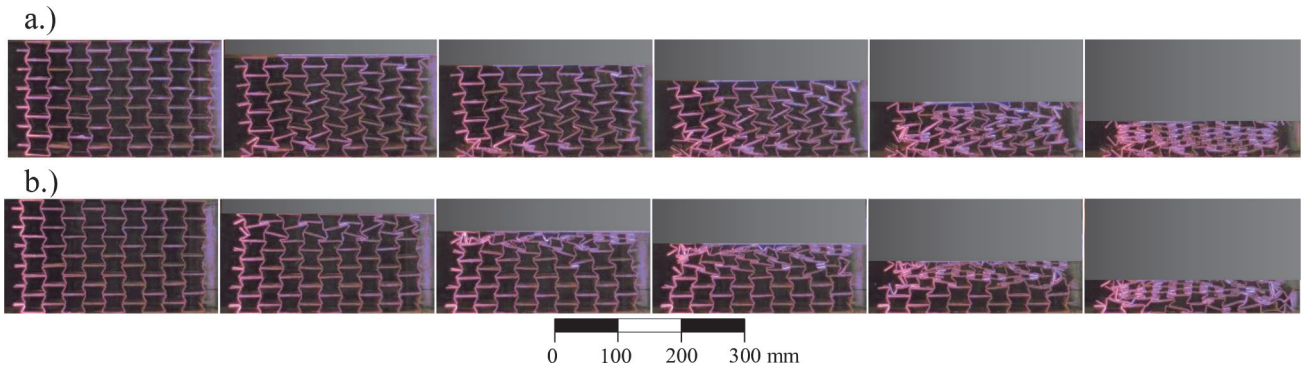

Fig. 5. Impact behaviour of two auxetic panels at different displacements (increments of 25 mm each), a) uniform AP 1.0 mm and b) graded panel.

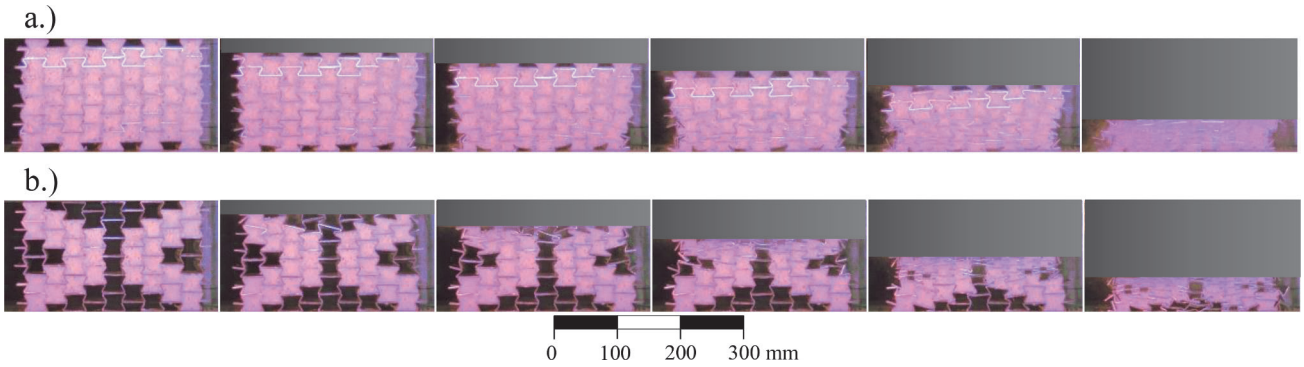

Fig. 6. Impact behaviour of two auxetic panels at different displacements (increments of 25 mm each), a) full-filled graded panel (FFG) and b) auxetic-filled graded panel (AFG).

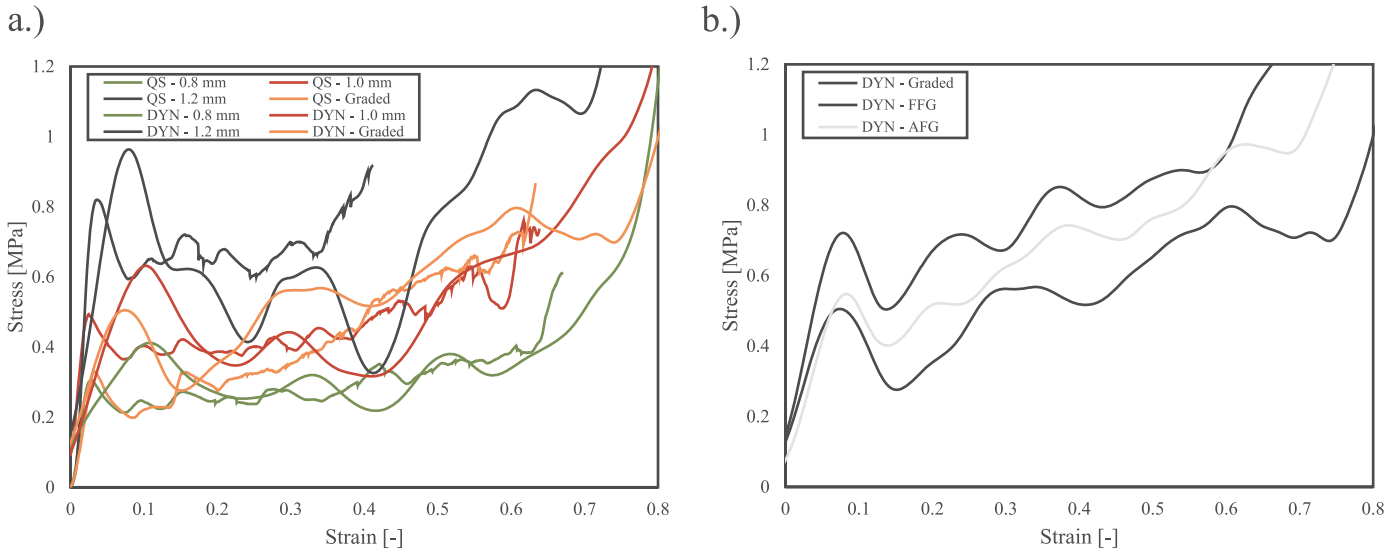

Fig. 7. Average mechanical response of a) non-filled and b) filled auxetic panels (compared to non-filled graded auxetic panel).

area of glue connections, which resulted in the different thicknesses of shell FE in these areas, as shown in Fig. 9a.

The loading conditions were modelled with two steel plates modelled with shell FE with 1 mm thickness and following material properties: Young's modulus 210,000 MPa, Poisson's ratio 0.3. In the case of quasi-static testing, the upper loading plate has a prescribed constant velocity of 2000 mm/s toward the sample. The increase of the loading velocity in FE model compared to the QS experimental tests was determined based on the parametric study to ensure the homogenous and quasi-static mechanical response without any inertia effect leading to the formation of the shock response. In the case of drop tower testing, the loading plate weighed 99.5 kg, and the initial velocity was prescribed the same as achieved in the experiments. The initial velocity in the case of the drop test was determined by the free fall equation and confirmed with the DIC from a high-speed video camera. The bottom support plate had fixed all degrees of freedom.

The computational model of FFG is shown in Fig. 9c, where the PU foam inserts were modelled with fully integrated solid FEs.

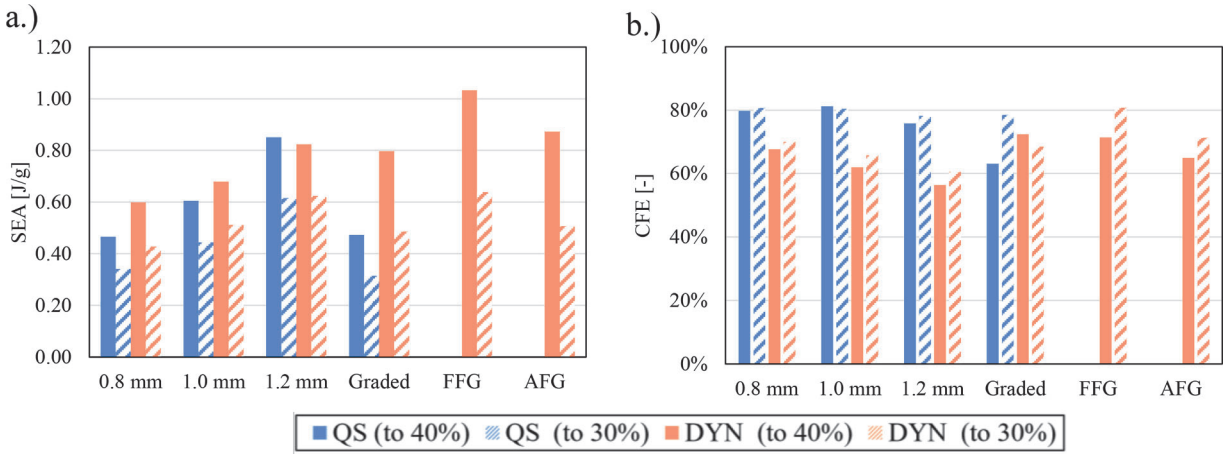

Fig. 8. Analysis of the experimental results, a) specific energy absorption (SEA) and b) crash force efficiency (CFE) of the considered auxetic panels evaluated up to 30% and 40% strain.

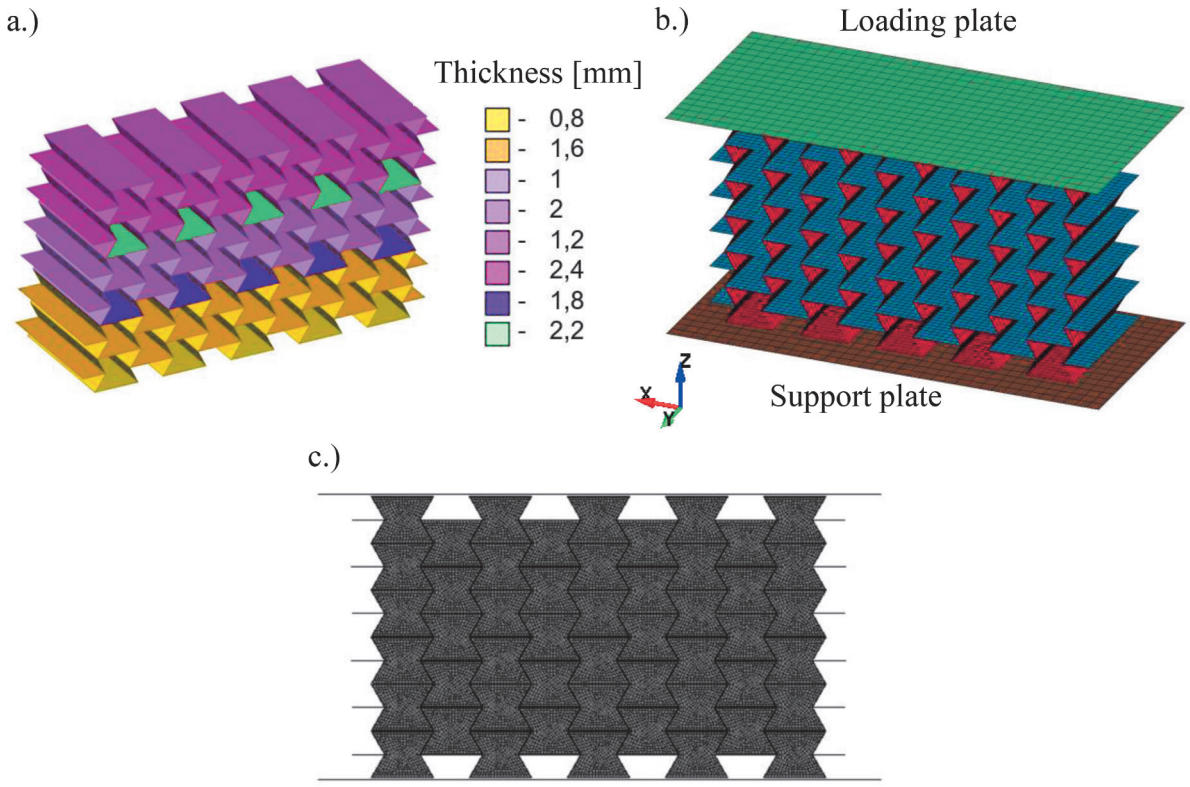

Fig. 9. Computational model of auxetic panel: a.) the thickness definition, b.) boundary conditions and c.) foam-filled FE model.

The *CONTACT_AUTOMATIC_NODES_TO_SURFACE contact was used between the plates and the auxetic panel and the auxetic panel and PU foam inserts, while the *CONTACT_AUTOMATIC_GENERAL was used for the contact between the shell FEs in the auxetic panel.

The shell FEs in the auxetic panel were modelled with elasto-plastic material model with strain hardening and rate dependence (MAT_024) based on the data from experimental testing (Fig. 3a). The volume FEs of PU foam inserts were modelled with crushable foam material model (MAT_063). The hardening behaviour (yield stress vs. volumetric strain) of the crushable foam material model was determined by the experimental tests (Fig. 3b), where the approximation curve with 50 data points was used to describe the simplified experimental curve. The material parameters were the same for quasi-static and dynamic loading and are given in Table 2. Additionally, the strain rate dependence of the AW 5754 was considered by using the Cowper-Symonds model with material parameters $c = 6500\ s^{-1}$ and $p = 4$ [69]. The temperature/adiabatic heat effects were not included in the material model.

4.2. Quasi-static testing results

The comparison between the experimental and computational quasi-static stress-strain results is shown in Fig. 10. Good agreement can be observed for all analysed geometries up to the densification. The largest discrepancy between the computational and experimental responses can be observed in the initial stiffness of the panels with thicker sheets. This can be consequence of the precise modelling of the panels in FE model, where the geometry is perfectly aligned together and therefore it starts to deform in predicted (auxetic) way at lower stress levels.

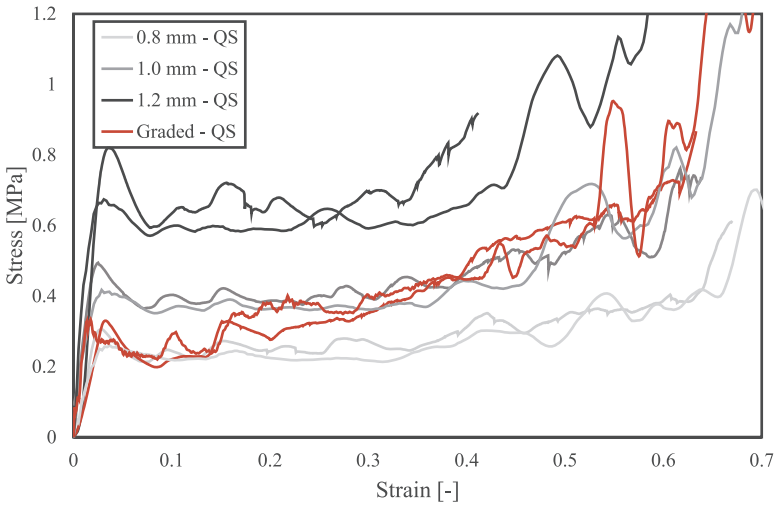

Fig. 10. Comparison of experimental (dashed lines) and computational (solid lines) results under quasi-static loading conditions.

The deformation behaviour comparison between the experiments and computational simulations is shown in Fig. 11, which also shows an excellent agreement.

4.3. Drop tower testing results

The mechanical responses of non-filled auxetic panel are shown in Fig. 12a, where good agreement can be observed between the experimental and computational results. In Fig. 12b the results of foam-filled auxetic panel are shown, again showing an excellent agreement between the experimental and computational results.

The quasi-static deformation behaviour of the uniform and graded samples is very similar. Therefore, only the results of AFG and FFG auxetic panels are graphically presented. Fig. 13 shows that the deformation is localised in the area of the thinnest sheets and then gradually moves to the areas with thicker sheets.

The transverse displacements of the points marked in Fig. 14a were measured in experimental results (DIC) and computational simulations to determine the Poisson's ratio. The initial alignment of the sample provides inadequate reading of the transversal displacement at lower strains, therefore the results up to strain of 0.1 are not representative. The results in Fig. 14b show that also foam-filled auxetic panels have a negative Poisson's ratio. An excellent agreement between the computational and experimental results is again evident. There is no significant difference between the AFG and FFG samples in terms of Poisson's ratio since the stiffness of the foam is much lower than the auxetic panel and does not influence the transversal deformation behaviour.

5. Conclusions

The auxetic panels were fabricated using the relatively cheap and straightforward fabrication method, which was extended by adding the PU foam to obtain foam-filled samples. The samples were tested under compression loading at two different loading velocities using the universal testing machine (quasi-static) and drop tower (dynamic). The mechanical properties of aluminium material and PU foam were also

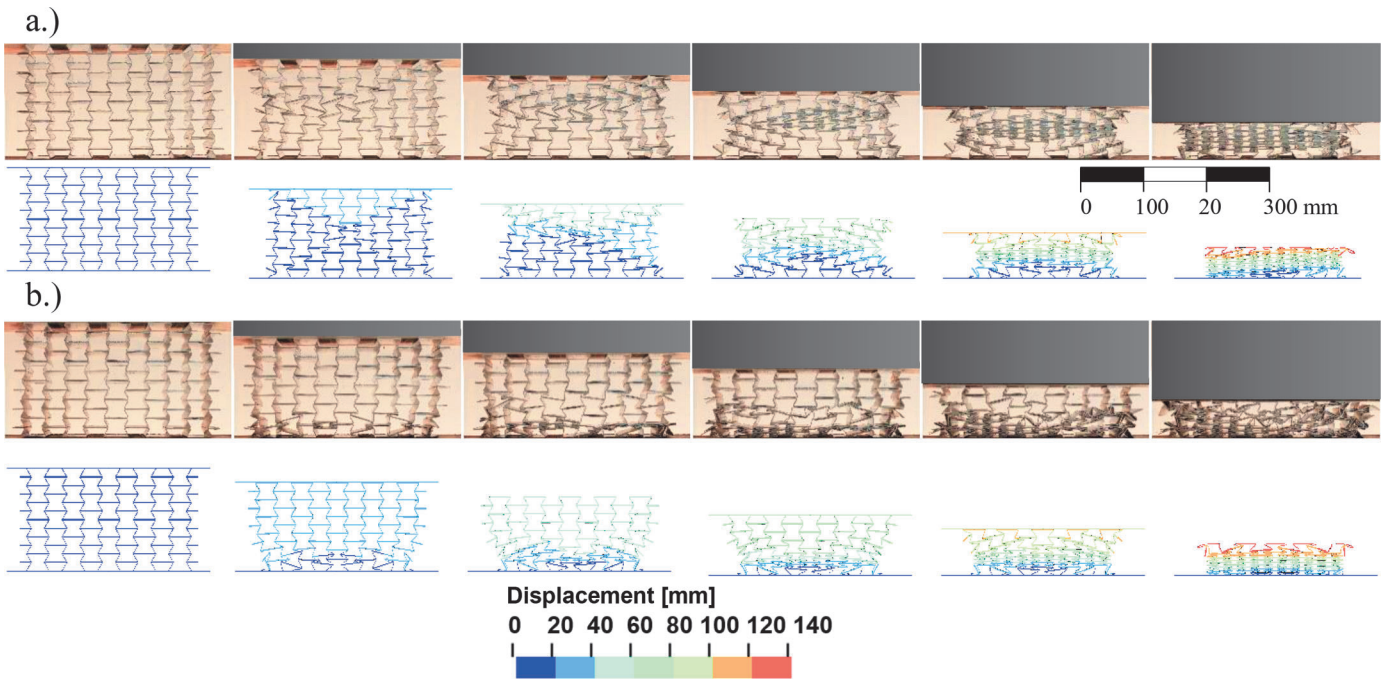

Fig. 11. Experimental and computational QS deformation behaviour of a) uniform AP 1.0 mm and b.) graded auxetic panel (displacement increment: 25 mm).

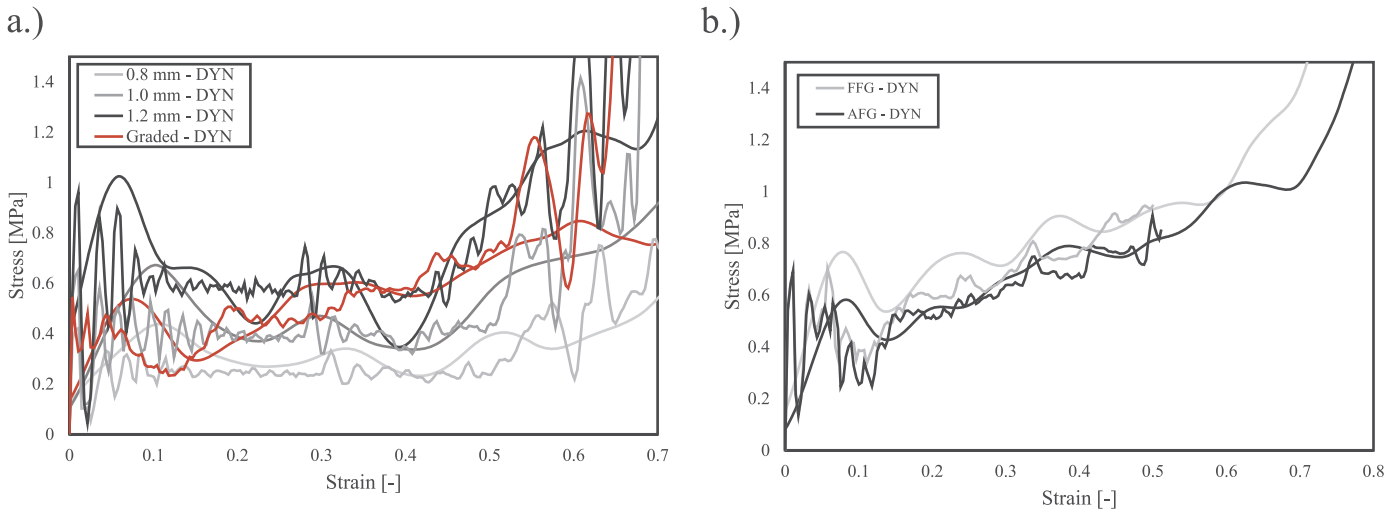

Fig. 12. Comparison of experimental (dashed lines) and computational (solid lines) stress-strain results of a) non-filled and b) foam-filled auxetic panel under dynamic loading conditions.

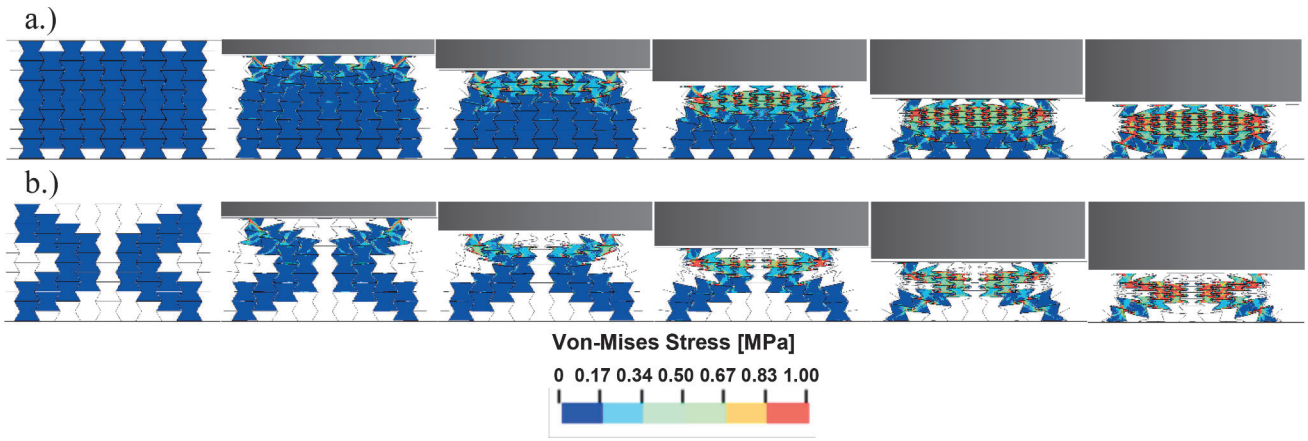

Fig. 13. Deformation behaviour of a) FFG and b) AFG auxetic panel under dynamic loading conditions.

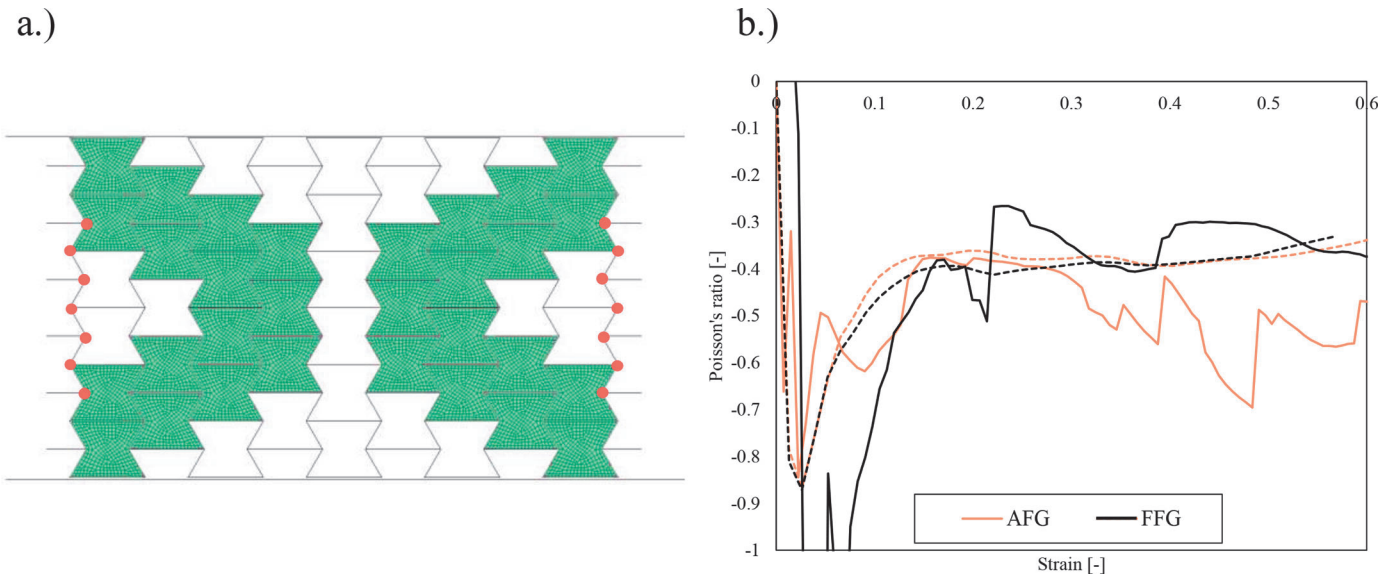

Fig. 14. DIC and numerical model displacement measuring points positions a.) and the Poisson's ratio values of AFG and FFG samples b.) (DIC – solid lines, computational simulations – dashed lines).

determined.

The mechanical testing reveals that the increase of the sheet thickness from 0.8 mm to 1.2 mm increases the SEA capabilities in the case of quasi-static and dynamic testing. The foam-filled auxetic panels increase the SEA capabilities even further and provide superior energy absorption capabilities compared to empty auxetic panels. The CFE, one of the crucial parameters in the crash absorbers, was also analysed. The CFE of uniform auxetic panels decreases in the dynamic loading compared to quasi-static case. The opposite was observed for graded auxetic panel, where the CFE remains comparable, also for the foam-filled samples.

The developed FE models successfully describe the mechanical and deformation behaviour. The DIC and the FE models confirmed that the auxetic panel provides the auxetic response up to very large strains. The FE models could be enhanced with the examination of the anisotropy and the real density distribution of PU foam, which will be considered in future work. The validated FE models enable the development of new foam-filled auxetic panels with a tailored response, where different geometries, sheet thicknesses, densities and distributions of the foams can be virtually tested before fabrication. This will hopefully lead to the application of modern crash absorption systems on newly built roads or blast protection elements in buildings.

Data availability

The data that support the findings of this study are available on request from the corresponding author.

CRediT authorship contribution statement

Nejc Novak: Conceptualization, Investigation, Writing – original draft. **Hasan Al-Rifaie:** Conceptualization, Investigation, Methodology, Writing – original draft. **Alessandro Airoldi:** Investigation, Methodology, Writing – review & editing. **Lovre Krstulović-Opara:** Investigation, Methodology, Writing – review & editing. **Tomasz Łodygowski:** Conceptualization, Funding acquisition, Resources, Writing – review & editing. **Zoran Ren:** Conceptualization, Funding acquisition, Supervision, Validation, Writing – review & editing. **Matej Vesenjak:** Conceptualization, Supervision, Validation, Writing – review & editing.

Declaration of Competing Interest

The authors declare that they have no known competing financial interests or personal relationships that could have appeared to influence the work reported in this paper.

Data availability

Data will be made available on request.

Acknowledgements

This research was funded by the Slovenian Research Agency fundamental postdoctoral research project (No. Z2-2648) and national research programme funding (No. P2-0063). The authors also gratefully acknowledge the support of companies Henkel Slovenija d.o.o and Bučar d.o.o.

References

[1] Jin X, Wang Z, Ning J, Xiao G, Liu E, Shu X. Dynamic response of sandwich structures with graded auxetic honeycomb cores under blast loading. Compos Part B Eng 2016;106:206–17.
[2] Al-Rifaie H, Studziński R, Gajewski T, Malendowski M, Sumelka W, Sielicki PW. A new blast absorbing sandwich panel with unconnected corrugated layers—Numerical study. Energies 2021;14:214.
[3] Novak N, Vesenjak M, Ren Z. Auxetic cellular materials-a review. Strojniški vestnik-J Mech Eng 2016;62:485–93.
[4] Novak N, Biasetto L, Rebesan P, Zanini F, Carmignato S, Krstulović-Opara L. Experimental and computational evaluation of tensile properties of additively manufactured hexa-and tetrachiral auxetic cellular structures. Add Manufact 2021;45:102022.
[5] Novak N, Krstulović-Opara L, Ren Z, Vesenjak M. Compression and shear behaviour of graded chiral auxetic structures. Mech Mater 2020;148:103524.
[6] Nowak Z, Nowak M, Pecherski R, Potoczek M, Sliwa R. Numerical simulations of mechanical properties of alumina foams based on computed tomography. Coupled Field Probl Multiphase Mater 2017:107.
[7] Andrews E, Sanders W, Gibson LJ. Compressive and tensile behaviour of aluminum foams. Mater Sci Eng A 1999;270:113–24.
[8] Pecherski RB, Nowak M, Nowak Z. Virtual metallic foams. Application for dynamic crushing analysis. Int J Multiscale Comput Eng 2017;15.
[9] Papadopoulos D, Konstantinidis IC, Papanastasiou N, Skolianos S, Lefakis H, Tsipas D. Mechanical properties of Al metal foams. Mater lett 2004;58:2574–8.
[10] Peroni L, Avalle M, Peroni M. The mechanical behaviour of aluminium foam structures in different loading conditions. Int J Impact Eng 2008;35:644–58.
[11] Gibson LJ, Ashby MF. Cellular solids: structure and properties. Cambridge university press; 1999.
[12] Dharmasena KP, Wadley HN, Xue Z, Hutchinson JW. Mechanical response of metallic honeycomb sandwich panel structures to high-intensity dynamic loading. Int J Impact Eng 2008;35:1063–74.
[13] Li X, Zhang P, Wang Z, Wu G, Zhao L. Dynamic behavior of aluminum honeycomb sandwich panels under air blast: experiment and numerical analysis. Compos Struct 2014;108:1001–8.
[14] Rathbun H, Radford D, Xue Z, He M, Yang J, Deshpande V. Performance of metallic honeycomb-core sandwich beams under shock loading. Int J Solids Struct 2006;43:1746–63.
[15] Hu L, Yu T. Dynamic crushing strength of hexagonal honeycombs. Int J Impact Eng 2010;37:467–74.
[16] Okumura D, Ohno N, Noguchi H. Post-buckling analysis of elastic honeycombs subject to in-plane biaxial compression. Int J Solids Struct 2002;39:3487–503.
[17] Zou Z, Reid S, Tan P, Li S, Harrigan J. Dynamic crushing of honeycombs and features of shock fronts. Int J Impact Eng 2009;36:165–76.
[18] Ruan D, Lu G, Wang B, Yu TX. In-plane dynamic crushing of honeycombs—A finite element study. Int J Impact Eng 2003;28:161–82.
[19] AL-RIFAIE H, Sumelka W. Auxetic Damping Systems for Blast Vulnerable Structures. In: Voyiadjis GZ, editor. Handbook of damage mechanics. II ed. Springer; 2020. p. 25.
[20] Xu S, Beynon JH, Ruan D, Lu G. Experimental study of the out-of-plane dynamic compression of hexagonal honeycombs. Compos Struct 2012;94:2326–36.
[21] Nia AA, Sadeghi M. The effects of foam filling on compressive response of hexagonal cell aluminum honeycombs under axial loading-experimental study. Mater Design 2010;31:1216–30.
[22] Hou X, Deng Z, Zhang K. Dynamic Crushing Strength Analysis of Auxetic Honeycombs. Acta Mechanica Solida Sinica 2016;29:490–501.
[23] Imbalzano G, Linforth S, Ngo TD, Lee PVS, Tran P. Blast resistance of auxetic and honeycomb sandwich panels: comparisons and parametric designs. Compos Struct 2017.
[24] Al-Rifaie H, Novak N, Vesenjak M, Ren Z, Sumelka W. Fabrication and mechanical testing of the uniaxial graded auxetic damper. Materials 2022;15:387.
[25] Yeganeh-Haeri A, Weidner DJ, Parise JB. Elasticity of or-cristobalitez A silicon dioxide with a negative Poisson's ratio. Science 1992;257:31.
[26] Zhang XY, Ren X, Zhang Y, Xie YM. A novel auxetic metamaterial with enhanced mechanical properties and tunable auxeticity. Thin-Walled Struct 2022;174:109162.
[27] Zhang M, Hu H, Kamrul H, Zhao S, Chang Y, Ho M. Three-dimensional composites with nearly isotropic negative Poisson's ratio by random inclusions: experiments and finite element simulation. Compos Sci Technol 2022;218:109195.
[28] Zhang X, Ding H, An L, Wang X. Numerical Investigation on Dynamic Crushing Behavior of Auxetic Honeycombs with Various Cell-Wall Angles. Adv Mech Eng 2015;7:679678.
[29] Alderson A. A triumph of lateral thought. Chem Ind 1999;17:384–91.
[30] Yang W, Li Z-M, Shi W, Xie B-H, Yang M-B. Review on auxetic materials. J Mater Sci 2004;39:3269–79.
[31] Greaves GN. Poisson's ratio over two centuries: challenging hypotheses. Notes Rec R Soc 2013;67:37–58.
[32] Liu Y, Hu H. A review on auxetic structures and polymeric materials. Sci Res Essays 2010;5:1052–63.
[33] Prawoto Y. Seeing auxetic materials from the mechanics point of view: a structural review on the negative Poisson's ratio. Compu Mater Sci 2012;58:140–53.
[34] Lira C, Innocenti P, Scarpa F. Transverse elastic shear of auxetic multi re-entrant honeycombs. Compos Struct 2009;90:314–22.
[35] Hou Y, Neville R, Scarpa F, Remillat C, Gu B, Ruzzene M. Graded conventional-auxetic Kirigami sandwich structures: flatwise compression and edgewise loading. Compos Part B Eng 2014;59:33–42.
[36] Schenk M, Guest SD, McShane GJ. Novel stacked folded cores for blast-resistant sandwich beams. Int J Solids Struct 2014;51:4196–214.
[37] Liu W, Wang N, Luo T, Lin Z. In-plane dynamic crushing of re-entrant auxetic cellular structure. Mater Design 2016;100:84–91.
[38] Scarpa F, Ciffo L, Yates J. Dynamic properties of high structural integrity auxetic open cell foam. Smart Mater Struct 2003;13:49.

[39] Grujicic M, Galgalikar R, Snipes J, Yavari R, Ramaswami S. Multi-physics modeling of the fabrication and dynamic performance of all-metal auxetic-hexagonal sandwich-structures. Mater Design 2013;51:113–30.
[40] Evans KE, Alderson A. Auxetic materials: functional materials and structures from lateral thinking! Adv Mater 2000;12:617–28.
[41] Scarpa F, Blain S, Lew T, Perrott D, Ruzzene M, Yates J. Elastic buckling of hexagonal chiral cell honeycombs. Compos Part A Appl Sci Manufact 2007;38:280–9.
[42] Miller W, Smith C, Evans K. Honeycomb cores with enhanced buckling strength. Compos Struct 2011;93:1072–7.
[43] Imbalzano G, Tran P, Ngo TD, Lee PV. A numerical study of auxetic composite panels under blast loadings. Compos Struct 2016;135:339–52.
[44] Hughes T, Marmier A, Evans K. Auxetic frameworks inspired by cubic crystals. Int J Solids Struct 2010;47:1469–76.
[45] Pikhitsa PV, Choi M, Kim HJ, Ahn SH. Auxetic lattice of multipods. Physica Status Solidi 2009;246:2098–101 (b).
[46] Bückmann T, Stenger N, Kadic M, Kaschke J, Frölich A, Kennerknecht T. Tailored 3D mechanical metamaterials made by dip-in direct-laser-writing optical lithography. Adv Mater 2012;24:2710–4.
[47] Lee JH, Singer JP, Thomas EL. Micro-/nanostructured mechanical metamaterials. Adv Maters 2012;24:4782–810.
[48] Remennikov A, Kalubadanage D, Ngo T, Mendis P, Alici G, Whittaker A. Development and performance evaluation of large-scale auxetic protective systems for localised impulsive loads. Int J Protect Struct 2019;10:390–417.
[49] Wang K, Chang Y-H, Chen Y, Zhang C, Wang B. Designable dual-material auxetic metamaterials using three-dimensional printing. Mater Design 2015;67:159–64.
[50] Shen J, Zhou S, Huang X, Xie YM. Simple cubic three-dimensional auxetic metamaterials. Physica Status Solidi 2014;251:1515–22 (b).
[51] Critchley R, Corni I, Wharton JA, Walsh FC, Wood RJ, Stokes KR. The preparation of auxetic foams by three-dimensional printing and their characteristics. Adv Eng Mater 2013;15:980–5.
[52] Al-Rifaie H, Sumelka W. The developement of a new shock absorbing Uniaxial Graded Auxetic Damper (UGAD). Materials 2019;12:2573.
[53] Zhang P, Liu J, Cheng Y, Hou H, Wang C, Li Y. Dynamic response of metallic trapezoidal corrugated-core sandwich panels subjected to air blast loading–An experimental study. Mater Design (1980-2015) 2015;65:221–30.
[54] Wiernicki CJ, Liem F, Woods GD, Furio AJ. Structural analysis methods for lightweight metallic corrugated core sandwich panels subjected to blast loads. Naval Eng J 1991;103:192–202.
[55] Studziński R, Gajewski T, Malendowski M, Sumelka W, Al-Rifaie H, Peksa P. Blast test and failure mechanisms of soft-core sandwich panels for storage halls applications. Materials 2021;12:70.
[56] Kalubadanage D, Remennikov A, Ngo T, Qi C. Experimental study on damage magnification effect of lightweight auxetic honeycomb protective panels under close-in blast loads. Thin-Walled Struct 2022;178:109509.
[57] Ajdari A, Nayeb-Hashemi H, Vaziri A. Dynamic crushing and energy absorption of regular, irregular and functionally graded cellular structures. Int J Solids Struct 2011;48:506–16.
[58] Zheng Z, Yu J, Li J. Dynamic crushing of 2D cellular structures: a finite element study. Int J Impact Eng 2005;32:650–64.
[59] Zhang Z, Lei H, Xu M, Hua J, Li C, Fang D. Out-of-plane compressive performance and energy absorption of multi-layer graded sinusoidal corrugated sandwich panels. Mater Design 2019;178:107858.
[60] Li S, Li X, Wang Z, Wu G, Lu G, Zhao L. Finite element analysis of sandwich panels with stepwise graded aluminum honeycomb cores under blast loading. Compos Part A Appl Sci Manufact 2016;80:1–12.
[61] Usta F, Türkmen HS, Scarpa F. High-velocity impact resistance of doubly curved sandwich panels with re-entrant honeycomb and foam core. Int J Impact Eng 2022;165:104230.
[62] Chen J, Zhu L, Fang H, Han J, Huo R, Wu P. Study on the low-velocity impact response of foam-filled multi-cavity composite panels. Thin-Walled Struct 2022;173:108953.
[63] Yang C, Chen Z, Yao S, Xu P, Li S, Alqahtani MS. Quasi-static and low-velocity axial crushing of polyurethane foam-filled aluminium/CFRP composite tubes: an experimental study. Compos Struct 2022:116083.
[64] Ren X, Zhang Y, Han CZ, Han D, Zhang XY, Zhang XG. Mechanical properties of foam-filled auxetic circular tubes: experimental and numerical study. Thin-Walled Struct 2022;170:108584.
[65] Haque Faisal N, Scott L, Booth F, Duncan S, McLeod A, Ghazi Droubi M. Effect of fillers on compression loading performance of modified re-entrant honeycomb auxetic sandwich structures. J Strain Anal Eng Design 2022:03093247221083210.
[66] Airoldi A, Novak N, Sgobba F, Gilardelli A, Borovinšek M. Foam-filled energy absorbers with auxetic behaviour for localized impacts. Mater Sci Eng A 2020;788:139500.
[67] Rudawska A, Wahab MA. The effect of cataphoretic and powder coatings on the strength and failure modes of EN AW-5754 aluminium alloy adhesive joints. Int J Adhesion Adhesives 2019;89:40–50.
[68] Novak N, Vesenjak M, Tanaka S, Hokamoto K, Ren Z. Compressive behaviour of chiral auxetic cellular structures at different strain rates. Int J Impact Eng 2020;141:103566.
[69] S.R. Bodner and P.S. Symonds, "Experimental and theoretical investigation of the plastic deformation of cantilever beams subjected to impulsive loading," 1962.